PROTEINS: Structure, Function, and Genetics 26:134–145 (1996)

Heptad Breaks in α-Helical Coiled Coils: Stutters and Stammers

Jerry H. Brown[1], Carolyn Cohen[1], and David A. D. Parry[2]
[1]*Rosenstiel Basic Medical Sciences Research Center, Brandeis University, Waltham, Massachusetts 02254-9110;*
[2]*Department of Physics, Massey University, Palmerston North, New Zealand*

ABSTRACT **The discontinuities found in heptad repeats of α-helical coiled-coil proteins have been characterized. A survey of 40 α-fibrous proteins reveals that only two classes of heptad breaks are prevalent: the stutter, corresponding to a deletion of three residues, and the newly identified "stammer," corresponding to a deletion of four residues. This restriction on the variety of insertions/deletions encountered gives support to a unifying structural model, where different degrees of supercoiling accommodate the observed breaks. Stutters in the hemagglutinin coiled-coil region have previously been shown to produce an underwinding of the supercoil, and we show here how, in other cases, stammers would lead to overwinding. An analysis of main-chain structure also indicates that the mannose-binding protein, as well as hemagglutinin, contains an underwound coiled-coil region. In contrast to knobs-into-holes packing, these models give rise to non-close-packed cores at the sites of the heptad phase shifts. We suggest that such non-close-packed cores may function to terminate certain coiled-coil regions, and may also account for the flexibility observed in such long α-fibrous molecules as myosin. The local underwinding or overwinding caused by these specific breaks in the heptad repeat has a global effect on the structure and can modify both the assembly of the protein and its interaction properties.**

Key words: α-fibrous proteins, supercoiling, structure prediction, hemagglutinin, mannose-binding protein, protein engineering

INTRODUCTION

As a result of recent crystallographic analyses of leucine zipper mutants,[1–3] the main structural features of α-helical coiled coils have become well characterized. In all cases the most striking aspect of the amino acid sequence of each chain is the heptad motif (*a, b, c, d, e, f, g*), where *a* and *d* are chiefly occupied by apolar residues. In two- and three-stranded coiled coils, this motif is repeated, on average, for 11–12 and 7 heptads, respectively.[4] An uninterrupted heptad repeat can be represented by separations of apolar residues alternatively three and four apart, that is, 3-4-3-4-3-4-3-4 (Fig. 1a). The small difference between the 3.5 residue average periodicity in the linear distribution of the apolar residues and the 3.6 residues per turn in an idealized right-handed α helix results in a left-handed supercoiling of the structure, which is accompanied by a shortening of the backbone hydrogen bond lengths for the core *a* and *d* residues.[5,6] The driving force for assembly is the necessity to remove apolar residues from the aqueous medium. The chains interact by forming an apolar core with "knobs-into-holes" packing[7]; this geometry characterizes the "perfect" coiled coil. In this structure, consecutive layers of interhelical contact are comprised of residues in *a* positions and residues in *d* positions, thus generating the so-called "*a* layers" and "*d* layers."[1] Each of these layers has its own distinguishing geometry, but both display knobs-into-holes close packing of apolar residues.

Tropomyosin was the first α-fibrous protein to be sequenced and is unique in many ways. The molecule displays an unbroken coiled-coil repeat more than 40 heptads in length. All other α-fibrous proteins either display discontinuities in the phasing of their heptad repeats or are much shorter in length. Some examples of the many α-proteins where these breaks occur include myosin and paramyosin, β-giardin from *Giardia lamblia,* apolipophorin III, apolipoprotein E3, trypanosome VSG, influenza hemagglutinin, omp α, intermediate filaments, lamin, M protein, gp 17, kinesin, NuMA, and fibrinogen. In all cases, these discontinuities are highly conserved, indicating their structural and functional significance. These proteins carry out many different functions and some (such as myosin, paramyosin, and intermediate filaments) assemble into filaments in the native state, whereas others exist as individual molecules.

In this article, we review the types of discontinuities that occur in coiled-coil sequences, and describe

Received January 2, 1996; revision accepted March 4, 1996.
Address reprint requests to Dr. Carolyn Cohen, Rosenstiel Basic Medical Sciences Research Center, Brandeis University, Waltham, MA 02254-9110.

their structural implications. This work is essentially an extension of the analysis by Lupas and colleagues,[8] but includes new data and interpretation derived from a detailed analysis of sequences with heptad repeats. Since there is as yet no high-resolution crystal structure for any α-fibrous protein, we rely mainly on established principles for coiled-coil packing, sequence information, and limited crystallographic data for (primarily homotrimeric) proteins with coiled-coil domains. We show that the types of discontinuities found in coiled-coil sequences are essentially limited to the previously identified deletion of three residues, the "stutter,"[9] and a newly identified deletion of four residues, referred herein as a "stammer." Their great prevalence argues for a unifying structural model where both sequence breaks can be accommodated in coiled coils with different degrees of supercoiling. We propose that specific non-close-packed cores, similar to those that mediate the transition across a stutter in an unwound coiled coil,[8] would also mediate the transition across a stammer in an overwound coiled coil. Based on a geometrical analysis of the main-chain coordinates of the homotrimeric coiled coils in hemagglutinin and mannose-binding protein, we also suggest that the accommodation of such heptad phase shifts is quite gradual and that the occurrence of non-close-packed cores in coiled coils may be more common than previously thought.

SKIPS, STUTTERS, AND STAMMERS

In principle, there are six distinct ways in which the heptad phasing can be disrupted: these correspond to deletions of 1, 2, 3, 4, 5, or 6 residues in an otherwise continuous repeat. (Note that deletions of n residues are equivalent to insertions of $7-n$ residues.) The identification of phase shifts in coiled-coil sequences has been made both by visual inspection and by computer programs. Two such programs, COILS (version 2.1)[8] and PAIRCOILS,[10] in general seek to maximize the occurrence of apolar residues in the a and d positions, but may do so by placing inappropriate residues elsewhere. We believe that visual inspection still has considerable merit over more automated methods of selecting regions with a heptad substructure.

In α-fibrous proteins thus far analyzed, deletions of three residues and insertions of one residue have been the two types of heptad phase shifts most commonly described.[6] The former correspond to so-called "stutters" and the latter to "skip" residues. (Note that, on this basis, a skip—equal to a deletion of six residues—is mathematically equivalent to two stutters.) In this paper, we also describe, for the first time, the "stammer," a deletion of four residues. Stutters, skips, and stammers represent apolar separations of 3-4-3-4-4-3, 3-4-(3+1)-4-3-4 or 3-4-3-(4+1)-3-4, and 3-4-3-3-4, respectively, in the sequence. Whenever a stammer occurs, the local average periodicity of apolar residues is reduced to less than 3.5. If a stutter occurs every 18 residues, then the local average periodicity of apolar residues increases to 3.6, and more closely matches the number of residues per turn in an idealized α helix.[8]

It can be argued that deletions of three and four residues would, in many respects, prove to be the least disruptive of the six listed previously, since they most closely match one turn of a helix (i.e., 3.6 residues) (Fig. 1). Thus, although the continuous left-handed stripe of apolar residues in the a and d positions is broken at the site of the deletion, the resulting azimuthal shift is quite small (~50° in both cases) (Fig. 1b, c). For the skip, the shift is twice as large (Fig. 1d). Previous analysis of the physical basis for stutters[8] has been based, in part, on the crystal structure of hemagglutinin.[11,12] Here, the close match between the number of residues per turn in an idealized α helix (3.6) and the average periodicity of apolar residues containing a stutter (~3.6) is accommodated by increasing the pitch of the supercoil (i.e., unwinding). This results in specific non-close-packed layers that mediate the transition across the stutter. An alternative model accommodates the stutter by introducing local but minor distortions within each of the constituent α helices.[13]

HEPTAD PHASE SHIFT SURVEY

We first sought to determine the prevalence of each type of possible heptad phase shift in naturally occurring coiled-coil sequences (Table I).[4,8,14–42] The database used consists of 30, 9, and 1 examples of 2-, 3-, and 4-stranded coiled-coil sequences, respectively, all of which contain discontinuities (defined here as six residues or less and not including a proline residue). Moreover, only those discontinuities having at least 21 coiled-coil residues at either end are included in this analysis. In addition, only one protein from each family is included in order to avoid biasing the data toward those families where many sequences have been completed. For those proteins with a repeating motif (such as spectrin or dynein), the data are entered for one repeat only. (In HPSR2, median body, and β-giardin, there is no exact sequence repeat, although there is a "fast Fourier transform" repeat of 25, 24, and 29 residues, respectively.) For the purpose of heptad phase-shift identification, amino acid residues were assigned heptad positions by visual inspection.

Using the methods described above, we find (Table I) that the six types of heptad phase shifts are not equally represented in coiled-coil discontinuities; rather, almost all shifts are restricted to stutters (three-residue deletions), skips (six-residue deletions, which, as we will argue, are two consecutive closely spaced stutters), and a newly identified disruption, which we call "stammers" (four-residue deletions). Differentiating between two closely spaced

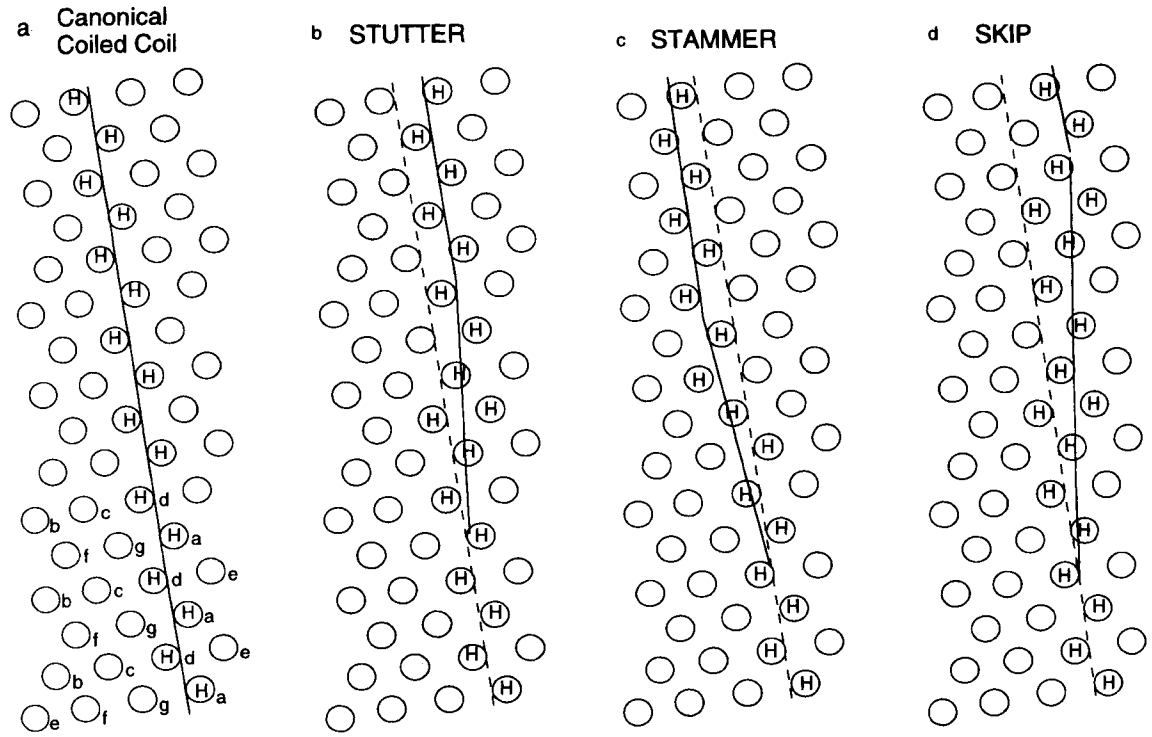

Fig. 1. Helix net diagrams showing the prevalent types of discontinuities in the heptad repeat of hydrophobic residues characteristic of coiled-coil domains. These diagrams are constructed by wrapping a (hypothetical) cylinder of paper around an idealized 3.6-residue-per-turn α helix, and marking with a circle the position of each side chain, as represented by its β-carbon atom.[7] The N terminus of each helix is on the bottom left. The solid line follows the course of residues (generally hydrophobic, marked by H) that interlock to form the core of the coiled coil. (**a**) Perfect heptad repeat throughout a canonical coiled coil. The heptad positions (*a, b, c, d, e, f, g*) are noted for the first 21 residues, and this pattern repeats continuously. (**b–d**) Heptad phase discontinuities that separate two segments of canonical coiled coil: (b) Stutter: three-residue deletion in the heptad repeat; (c) Stammer: four-residue deletion; (d) Skip: two closely-spaced three-residue deletions. The N-terminal 21 residues in these diagrams are "aligned" with those in (a), and the dashed lines show the continuation of the perfect heptad repeat for comparison. The difference between the dashed and solid lines at the top of the figures represent the azimuthal shifts that accommodate the heptad phase shifts (approximately 50°, −50°, and 100° for the stutter, stammer, and skip, respectively, but the precise values depend critically on the coiled-coil and α-helix parameters). For any given discontinuity, the smaller the difference between the slope of the solid line, which traverses the phase shift, and the slope of the (dashed) line in the perfect heptad repeat, the longer the axial extent over which the phase shift will be traversed.

stutters (i.e., 4-3-4-4-3-4-3-4-4-3) and a skip ((4-3-4-3-4-(3+1)-4-3-4-3) or (4-3-4-3-4-3-(4+1)-3-4-3)) on the basis of primary sequence information can be somewhat arbitrary.[†] Either type of heptad phase shift would cause core packing discontinuities. Moreover, as shown below, stutters can be accommodated in a continuous helix; in contrast, the insertion of one residue (a true skip) would necessarily cause a break in the helix (see, for example, the structure of the GreA transcript cleavage factor[44]). In general, skips and stutters can readily be distinguished only if the three-dimensional structure is available. We expect most of the skips in Table I to correspond to two stutters too closely spaced in sequence to be separated. The data indicate that while discontinuities other than stutters (or skips) and stammers may also occur, they are extremely rare.

[†]The difficulty in distinguishing between a skip and two stutters by sequence alone can be illustrated by the following examples:

Two closely spaced stutters	One skip
a b c d* e f g*	*a* b c d* e f g*
a b c d* e f g*	*a* b c d* e f g*
d e f g a* b c*	*a* b c d* e f g*
g a b c d* e f*	*g a* b c d* e f*
g a b c d* e f*	*g a* b c d* e f*
g a b c d* e f*	*g a* b c d* e f*

where * represents an apolar residue. In this illustration only one apolar residue is in a different position. Bearing in mind that positions *a* and *d* are occupied only about 75% of the time by apolar residues, it becomes clear that sequence analysis cannot distinguish between two closely spaced stutters and a skip. In the program COILS,[8] use of smaller sized scanning windows can convert skips into stutters. Also, in the homotrimeric coiled-coil of hemagglutinin, the heptad phase shift has been described both as a skip[43] and stutters.[8] Inspection of the three-dimensional structure[11] shows them to be stutters.

TABLE I. Stutter (−3), Stammer (−4), and Skip (−6) Database*

Coiled coil sequences	+1/−6	+2/−5	+3/−4	+4/−3	+5/−2	+6/−1
Two-stranded						
Myosin[14]	5	0	0	0	0	0
Paramyosin[15]	4	0	0	0	0	0
IF proteins[16] (except lamin)	0	0	0	1	0	0
Lamin[17]	1	0	0	1	0	0
Desmoplakin[18]	0	0	1	1	0	0
BPA[18]	0	1	1	1	0	0
Plectin[19]	3	0	2	0	0	0
M6[20]	1	0	1	5	0	0
CG-1[21]	1	0	5	5	0	0
NuMA/centrophilin[22]	2	0	0	4	0	0
NUF1[23]	2	0	0	1	0	0
NUF2[24]	1	0	0	2	0	0
CIK1[25]	2	0	0	2	0	1
Kinesin[26]	0	0	1	2	0	0
Dynein[27]	1	0	0	0	0	0
Pericentrin[28]	2	0	0	5	0	0
SF-assemblin[29]	6	0	0	1	0	0
Kinesin-like protein[30]	1	0	1	1	0	0
β-Giardin[31]***	7***	0	0	1	0	0
Median body[32]**	0	1	19**	1	0	0
HPSR2 head stalk[33]*	0	1	1	45*	0	0
sec2[34]	1	0	1	0	0	0
SMC1[35]	3	0	0	3	0	0
gp wac[36]	0	0	0	0	1	0
Cell att protein/reovirus[37]	0	0	0	1	0	0
Salmonella typhimurium[38]	1	1	0	0	0	0
USO1 (yeast)[39]	1	0	2	9	0	1
R07E5.6 C elegans[40]	0	0	1	0	0	0
Bicaudal protein[41]	1	0	3	0	0	1
tpr protein[42]	1	0	2	4	0	0
Total	47***	4	41**	96*	1	3
Three-stranded						
Laminin A[4]	0	1	0	0	1	1
Laminin B1[4]	2	1	1	0	0	0
Laminin B2[4]	0	0	0	1	0	1
gp17[4]	0	0	0	1	0	0
Spectrin[4]	0	0	0	0	0	1
MSRP[4]	0	0	0	1	0	1
αFBN[4]	1	0	0	0	0	0
βFBN[4]	0	0	0	0	1	0
γFBN[4]	0	0	0	1	0	0
Total	3	2	1	4	2	4
Four-stranded						
Omp α[8]	2	0	0	5	0	0
Total	2	0	0	5	0	0

*Proteins denoted with asterisks have inexact sequence repeats (see text).

UNDERWOUND COILED-COIL MODEL OF THE STUTTER

One approach to analyze the effect of the stutter—that might also account for the restrictions on the types of naturally occurring heptad breaks—is to model the topology of the interactions between residues lying along the contact line between the α helices. This analysis was carried out by Lupas and colleagues,[8] who, instead of introducing local deformations within the constituent α helices, accommodate the stutter by reducing the degree of supercoiling of the α helices, that is, by allowing the pitch length of the coiled coil to increase over an axial distance of about two to four turns. In the regular left-handed supercoil associated with noninterrupted heptad repeats, the side chains at every 7.0 residues (less than 2 turns of an idealized α helix) face toward the other helix (or helices) of the coiled coil (Fig. 2); in contrast, in the underwound coiled coil—postulated here to occur in the vicinity of stutters—the side chains at approximately every 7.2 residues (two turns of an idealized α helix) face in

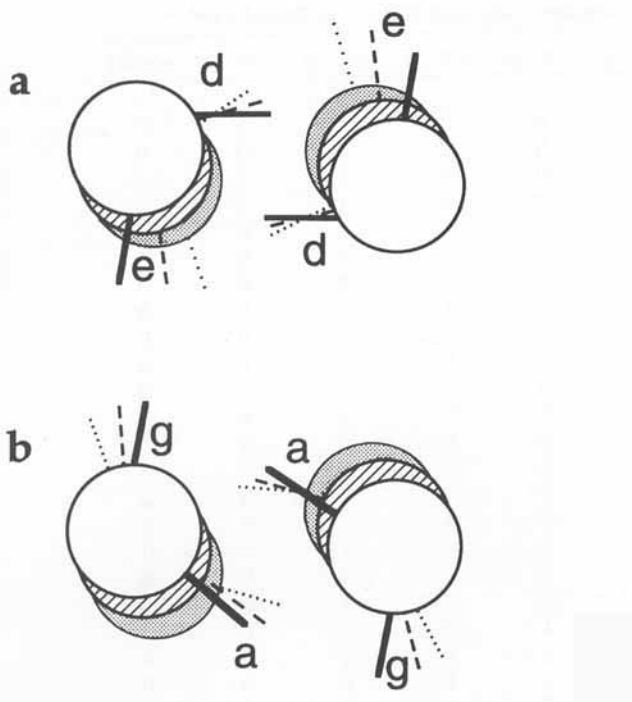

Fig. 2. Schematic diagram of the core residues of three heptads in a left-handed dimeric coiled coil, corresponding to an uninterrupted heptad repeat. The circles correspond to consecutive sections of the main chain, and the lines emanating from them represent side chains. The dimer axis is perpendicular to the plane of the paper. Solid lines show nominal knobs-into-holes close-packed cores. Dashed and dotted lines represent, respectively, layers 7 and 14 residues further along the sequence. These residues are in equivalent positions relative to the coiled-coil axis and display the same knobs-into-holes packing due to a crossing angle between the helices of ~20° and a pitch length of ~140 Å[1,7] (**a**) *d* layers: *d* residue side chains from one helix point into the "holes" between the *d* and *e* side chains of the facing helix. (**b**) *a* layers: *a* side chains from one helix point into the holes between the *a* and *g* side chains of the facing helix.

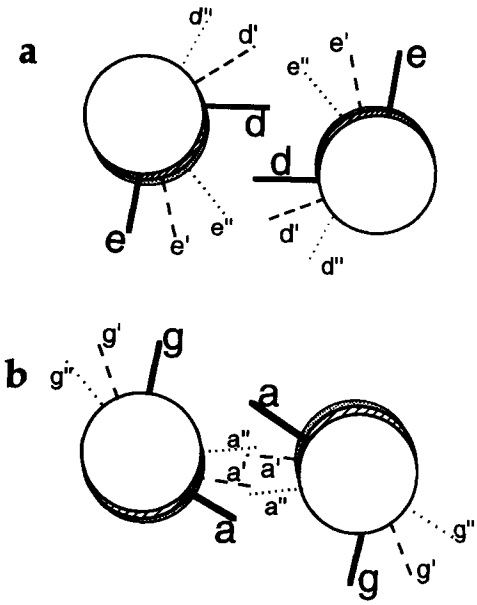

Fig. 3. Schematic diagram of the core residues of three heptads in a partially unwound dimeric coiled coil, corresponding to an arrangement that accommodates a stutter. Side chains separated by 7 or 14 residues are not in equivalent positions relative to the coiled-coil axis, and are denoted differently (x, x,', x"). (**a**) The *d* layer (solid lines) is transformed via a "*d/a*" layer (dashed lines) into an *a*-type layer (dotted lines; cf. Fig. 2b). (**b**) The *a*-layer (solid lines) is transformed via an "a/d" layer (dashed lines) into a *d*-type layer (dotted lines; cf. Fig. 2a). Note that these intermediate *d/a* and *a/d* layers in dimeric coiled coils generally form four-residue and two-residue non-close-packed cores, respectively. Also note that the position of the back circle, and therefore any structure following this unwound segment, is shifted clockwise about the coiled-coil axis relative to that in the canonical coiled coil of Figure 2.

the same direction (Fig. 3). Such an unwinding of the supercoil has quite specific effects on the packing of residues along the axial line of contact between the constituent α helices.

In a perfect coiled coil, all of the interactions between the helices involve knobs-into-holes packing[1,7]: the side chains of the *d* residues, for example, in one α helix point directly toward the hole formed between the side chains of residues in the *d* and *e* positions in an adjacent helix (Fig. 2a). If, however, the helices are not supercoiled, then a residue seven positions from a nominal *d* residue (d' in Fig. 3a) would point approximately at the residue seven positions from the nominal *e* residue (*e'*) in an adjacent α helix. This orientation gives rise to a non-close-packed core (dashed lines in Fig. 3a), depending on the precise side-chain conformation and the local interhelical radii. If the α helices continue to run approximately parallel for a further heptad, then the packing of the side chains 14 residues from the nominal *e* residues (dotted lines in Fig. 3a) begins to resemble that of residues in nominal *a* layers. In this scheme the *d* layer is gradually transformed into an *a* layer, and an intermediate and "imperfect" form of side-chain packing between the helices occurs. This side-chain arrangement has been referred to as a *d/a* layer[8] (dashed lines in Fig. 3a) and leads to a hole at the axis of the coiled-coil rod.

By a similar argument, we may also consider what happens to the packing of the residues in the *a* layers. The side chains in nominal *a* residues point toward the holes formed between the side chains of residues in the *a* and *g* positions of an adjacent α helix (Fig. 2b). If the chains are not supercoiled about one another, then the residues seven positions after nominal *a* residues in both chains would point directly at one another (dashed lines in Fig. 3b). After another heptad (dotted lines), the residues begin to resemble those in the *d* layer. In the unsupercoiled structure, as an *a* layer is transformed into a *d* layer, another non-close-packed arrangement could occur. In this so-called "*a/d* layer" (dashed lines in Fig. 3b) (called an "x" layer in ref. 8), side chains from the helices interact at the axis of the coiled coil, thus giving rise to a different packing

from the *d/a* layer. If the helices are just slightly supercoiled about one another (i.e., slightly underwound from the perfect coiled coil in Fig. 2), then the transformation through the stutter would be more gradual, and more intermediate *d/a*-like and *a/d*-like layers would occur (see below). The accommodation of stutters by the use of *d/a* and *a/d* layers is observed for the homotrimeric coiled coils in hemagglutinin[8,12,45] and in the rat mannose-binding protein (see below) where unwinding of the coiled coils compensates for the relatively small difference between the 3 residues deleted in a stutter and the 3.6 residues in one turn in an idealized α helix.

OVERWOUND COILED-COIL MODEL OF THE STAMMER

The same general approach of systematically altering the nature of the apolar residue interactions between the helices can be adopted to model the stammer. Here the relatively small difference between the heptad phase shift arising from the 4-residue deletion and the 3.6 residues per turn in an α helix can be accommodated by further supercoiling, that is, decreasing the pitch length from that found in a "perfect" coiled coil, instead of the decreased supercoiling found for stutters. The same non-close-packed *d/a* and *a/d* structures would form as the stammer is traversed.

Just as we described how the intermediate *d/a* and *a/d* structures form for stutters in an underwound coiled coil (Fig. 3), we may similarly outline how they form for stammers in an overwound coiled coil (Fig. 4). Here, the side chains of residues seven positions from nominal *d* residues would point approximately right at each other forming the "*a/d*" (or x) non-close-packed structure (dashed lines in Fig. 4a). Residues 14 positions from the nominal *d* residues (dotted lines) would begin to resemble *a* layers. Similarly, side chains of residues seven positions from nominal *a* residues would point at the side chains 7 positions from nominal *g* residues, forming the "*d/a*" non-close-packed structure (dashed lines in Fig. 4b). After another heptad, the residues begin to resemble *d* layers. Marginally less overwinding than that shown in Figure 4 would make the transformation through the stammer more gradual.

In contrast to the underwound model for the stutter, the overwound model of the stammer is a hypothetical structure that is currently without direct experimental verification. As seen in Table I, stammers, though prevalent, are found considerably less frequently than stutters. Overwinding of the coiled coil, with a concomitant shortening of the backbone hydrogen bond lengths of the core residues, would be expected to place a somewhat greater strain on the backbone integrity of the α helices than underwinding, where the helices are actually straighter than in the nominal coiled coil. In fact, although six-residue-deletion skips [equivalent to two closely spaced stutters and requiring possibly significant (local) underwinding] are quite prevalent, one-residue deletions [equivalent to two closely spaced four-residue-deletion stammers, requiring possibly significant (local) overwinding] are very rare. It appears, therefore, that shifts in the heptad repeats of apolar residues in coiled-coil domains are predominantly those that minimize the deformations of the constituent helices.

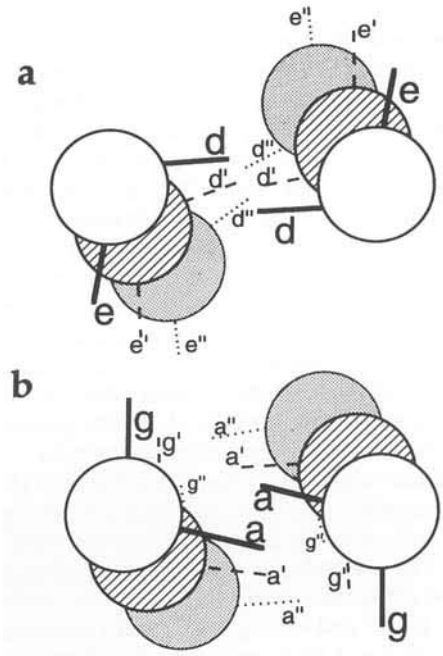

Fig. 4. Schematic diagram of the core residues of three heptads in an overwound left-handed dimeric coiled coil, corresponding to an arrangement proposed to accommodate a stammer. (**a**) The *d*-layer (solid lines) is transformed, here via an "*a/d*" layer (dashed lines), into an *a*-type layer (dotted lines). (**b**) The *a*-layer (solid lines) is transformed via a *d/a* layer (dashed lines) into a *d*-type layer (dotted lines). Note how the use of the *a/d* and *d/a* intermediates in transforming between the canonical *a* and *d* layers would be reversed in the stammer relative to the stutter. Also note that the position of the back circle, and therefore any structure following this overwound segment, is shifted counterclockwise about the coiled-coil axis relative to that in the canonical coiled coil of Figure 2.

GLOBAL CONSEQUENCES OF LOCAL UNDERWINDING OR OVERWINDING

Following the underwound or overwound region of coiled coil that would accommodate a heptad phase shift, normal supercoiling could resume provided that the heptad period is maintained without further disruption. In such models, however, the relative position of any particular residue in the coiled-coil segment following the region of the heptad break would be different from the case in which no heptad phase shift had occurred. For example, if we were to overlay the structures in Figures 2, 3, and 4

such that the N-terminal residues (front circles) were perfectly aligned, then the C-terminal residues (back circles) and all subsequent residues would be rotated about the coiled-coil axis clockwise in the underwound stutter (Fig. 3) and counterclockwise in the overwound stammer (Fig. 4) relative to the equivalent residues following an uninterrupted coiled coil (Fig. 2). The precise degrees of rotation about the coiled-coil axis would depend on the specific coiled-coil and α-helical parameters, but they derive from the need to traverse the approximately 50° between the radially nearest residues within a heptad of an α helix (Fig. 1). Accommodation of these heptad phase shifts by local alterations in the degree of supercoiling would therefore produce global changes in the structure of the protein.

Alternatively, to accommodate a break in the heptad repeat without global consequences, the constituent α helices would necessarily become locally distorted. For example, in order to internalize apolar residues along the coiled-coil axis in the vicinity of a stutter, North and colleagues[13] used a simulated annealing protocol that restricted the distribution of structural deformations to just the two turns of α helix (essentially one heptad) closest to the deletion. With this approach, however, we would have no reason a priori to expect any restrictions on the types of heptad phase shifts found in coiled coils, since, in theory, it should be possible to accommodate any heptad discontinuity with an appropriate α-helical deformation. In contrast, the model of accommodating discontinuities in coiled coils by small differences in the degree of supercoiling accounts well for the observation that only certain heptad phase shifts occur in practice. For example, the one-residue deletion (equal to two closely spaced stammers), which, in this model, would be highly overwound, is not found (Table I). Moreover, since this model predicts that mutations that cause heptad phase shifts would necessarily have global consequences for the structure of the protein, we would expect and do observe that heptad discontinuities exhibit high degrees of conservation.

UNDERWINDING OBSERVED IN HOMOTRIMERIC COILED COILS

We have reviewed how the accommodation of heptad phase shifts yields coiled-coil regions with nonideal geometry for knobs-into-holes packing. For a complete traversal of a stutter, for example, this model requires a net unwinding of ~50°; this analysis does not, however, specify the axial extent of the coiled coil over which the unwinding occurs. If the stutter is traversed in a relatively short stretch of highly underwound coiled coil (as is shown in Fig. 3), then much of the structure remains in ideal position for knobs-into-holes packing. On the other hand, if the stutter is traversed over a longer stretch of slightly underwound coiled coil, then more intermediate *d*/*a*-type and *a*/*d*-type layers will be formed.

In order to determine how gradually a stutter is traversed, we have analyzed the main-chain geometry of the core residues in crystallographically determined high-resolution homotrimeric coiled-coil structures. The method we used relies on measuring the average of angles made between certain vectors defined by combinations of main-chain atoms from the same residues on facing helices (Fig. 5, left, and caption for details). Averaging over different pairs of main-chain atoms, to smooth out the effects of coordinate errors,[46] allows the core positions to be quantitatively distinguished from one another: thus *e* residues have the largest average angle, followed by *a* residues, then *d* residues, and *g* residues with the smallest average angle. Note that related previous analyses[43,46] have examined supercoiling by determining pitch values, where dihedral angles between main-chain coordinates on distant residues along the coiled coil are calculated; by contrast, our method uses coordinates from residues at the same level and yields a numerical description of the different types of heptad positions. Thus, displaying the average angles for every seventh residue is a measure of how gradually one type of layer is transformed into another type of layer across a heptad break, and quantifies features observed in ribbon (Fig. 5, middle) and stick diagrams (Fig. 5, right).

Before applying this method to hemagglutinin, which contains stutters, we analyzed the rat mannose-binding protein (PDB code 1RTM)[47] and GCN4-pII (T. Alber, personal communication).[3] Both of these latter proteins are homotrimeric coiled coils whose coordinates have recently become available. The heptad repeat in GCN4-pII is uninterrupted, and a one-residue insertion has been reported for the homologous coiled coil of human mannose-binding protein.[48] For a perfect coiled coil, the main-chain average angles for a set of *e, a, d,* and *g* residues within one heptad would be roughly the same for all like positions throughout the coiled coil, and this result was observed for the artificially designed GCN4-pII (note relatively flat lines in Figure 5A, left). In contrast, the average angle underwent a clear (downward) shift for consecutive heptad positions in the rat mannose-binding protein coiled coil (e.g., the values for *e* positions 75, 82, 89, and 96 are 88.5°, 84.5°, 81.9°, and 78.4°, respectively) (Fig. 5b, left). These data indicate that GCN4-pII residues follow a relatively uninterrupted heptad repeat, but that rat mannose-binding protein "*e*" position 96 has partial *a* character, "*a*" position 99 has partial *d* character, and "*d*"-position 95 has partial *g* character, according to the geometry of their main-chain atoms. The models discussed above (Figs. 2, 3), suggest that these results are consistent with a relatively canonical coiled coil for GCN4-pII (Fig. 5a,

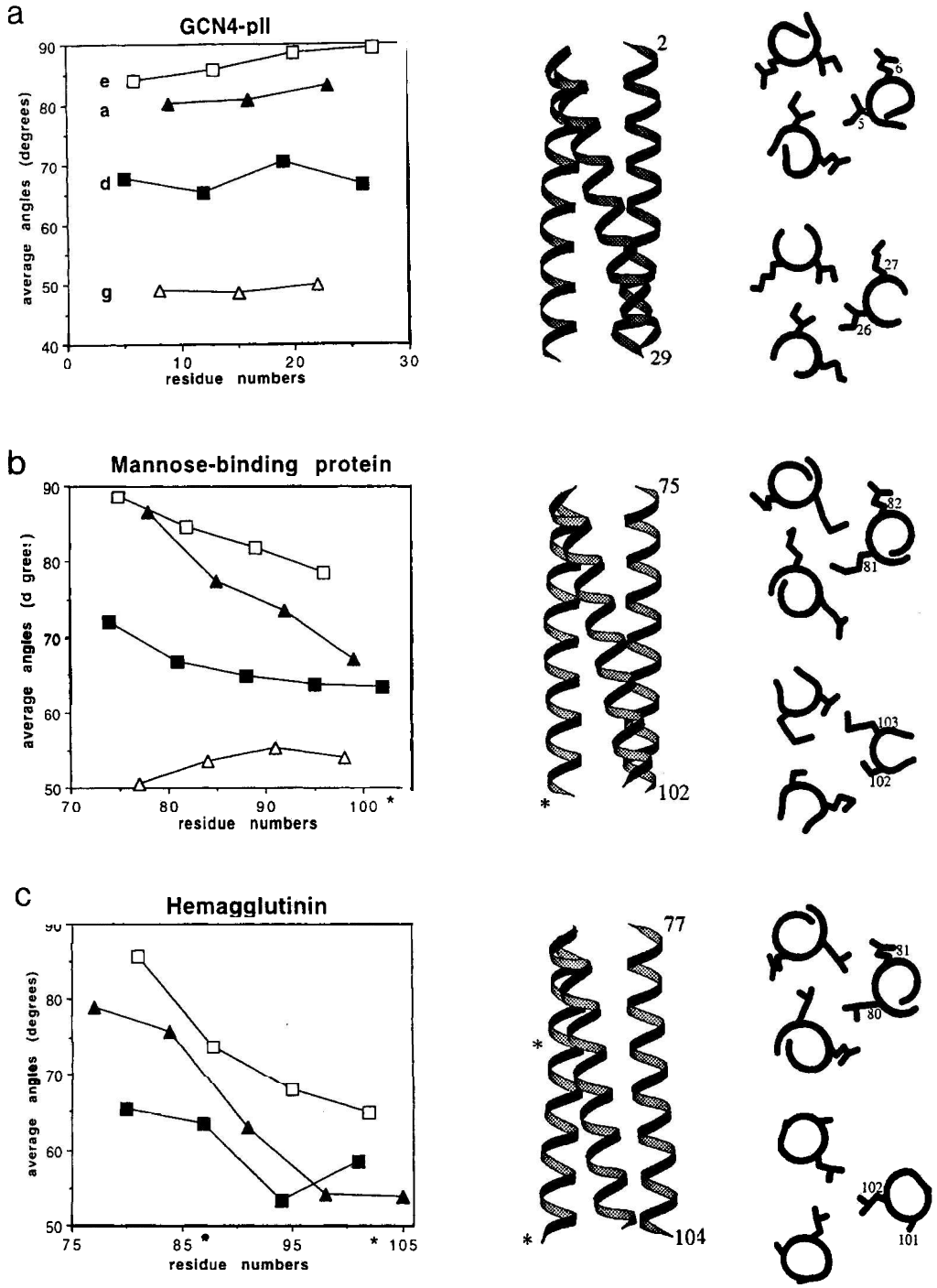

Fig. 5. "Average-angle" measurements (*left*), ribbon diagrams (*middle*), and side-chain packing views (*right*) in homotrimeric coiled coils. The geometric identification of core residues (*left*) is based on measuring the angles between vectors defined by certain combinations of main-chain atoms on one helix and like vectors on the facing helix. The specific combination chosen here, the average of the inter N→Cα angle, the inter C→O angle, and the Cβ→Cα to Cα→Cβ angle, quantitatively distinguishes between different core residues more precisely than does any individual measure. The mean of the three interhelical average angles for each residue is displayed here. Every 7th residue is connected by a line, and -□-, -▲-, -■-, and -△- represent those heptad groups whose N termini residues occupy *e, a, d,* and *g* positions, respectively; • indicates the approximate center of a stutter. The ribbon diagrams (*middle*) are 28-residue segments of coiled coil oriented such that their N termini coincide (as visualized at the *top left*). Differences between them can be most easily visualized at the *bottom right.* Note that as the helices adopt a more parallel disposition to one another (larger pitch), the axial distance required to traverse one stutter decreases. The side-chain packing diagrams (*right*) are viewed perpendicularly to the ribbon diagram, looking down from the N terminus toward the C terminus and then rotated such that the general locations of the helices relative to the page would coincide. For each protein, the top diagram is a *d* layer near the N terminus of the coiled coil and the bottom diagram shows the disposition of the side chains exactly 21 residues away, that is, three heptads. (**a**) GCN4-pII (T. Alber, personal communication). Note that consecutive heptad positions maintain the same main-chain geometry: the flat average-angle profile (*left*) and the near coincidence of the Cα-Cβ vectors for residues 5 and 26 (*right*). This perfect heptad repeat yields the left-handed supercoiling shown in the ribbon diagram (*middle*). (**b**) Rat mannose-binding protein (PDB code 1RTM). The slightly underwound coiled coil (*middle*) results in a shift in the main-chain geometry for consecutive heptads (*left*) such that a *d/a* layer is formed by residues 102 and 103 (*right*). (**c**) Hemagglutinin (coordinates refined against data from flash-frozen crystal; S. Watowich, personal communication). The highly underwound coiled coil (*middle*) results in large changes in the main-chain geometry from one heptad to the next (left). A *d/a* layer at residues 87 and 88 (see Figure 6) and an *a/d* layer at residue(s) (101 and) 102 are found one and three heptads, respectively, from the *d* layer at residues 80 and 81 (*right*).

middle) and a slightly underwound coiled coil associated with a stutter for rat mannose-binding protein (Fig. 5b, middle). The helical main chains in mannose-binding protein are configured such that the transformation from layer to layer preceding the stutter is gradual and extends over a number of heptads.

The disposition and apolar character of the side chains in the coiled coil of mannose-binding protein promote the gradual underwinding associated with the heptad phase shift. Residues 102 and 103 contact each other in a tip-to-tip manner as in a *d/a* layer (Fig. 5b, right). This non-close-packed structure occurs at the C terminus of the coiled coil. Examination of the residue types in the *e* positions is also indicative of the heptad phase shift. One would also predict that as *e* residues gradually take on more "*a*"-like character, their side chains would become more hydrophobic. This feature in fact occurs in mannose-binding-protein sequences (Fig. 8 in ref. 47), where *e* positions 75 and 82 are composed of glutamic acid, aspartic acid, and alanine (side chains with small hydrophobic regions), *e* positions 89 and 96 are composed of asparagine, glutamine, lysine, and arginine (the latter two having relatively substantial hydrophobic regions), and "*e*" position 103 is composed of the exclusively hydrophobic methionine and leucine side chains. This gradual shift in the apolar content of residues in the heptad repeat thus provides a stabilizing hydrophobic core in the C-terminal region of the mannose-binding protein coiled coil.

In agreement with previous analyses that have established the existence of a stutter at position 87/88 of hemagglutinin,[8] we do in fact observe shifts in the main-chain based average angles for the two consecutive heptad positions surrounding this stutter (Fig. 5c). Furthermore, as in the case of the mannose-binding protein, this shift is rather gradual. On one side of the 87/88 stutter, *a* position 84 has more "*d*"-like character than does *a* position 77; but on the other side of this stutter and before the next stutter at 102→105/106, *d* position 98 has more "*g*"-like character than *d* position 91. The side chains of 102 and 105/106 form non-close-packed *a/d* (Fig. 5c, right) and *d/a* layers, respectively, at the C terminus of the coiled coil.

This quantitative analysis demonstrates that—for the trimeric coiled coils studied here—consecutive heptad layers, including those between previously identified stutters, are not geometrically identical but follow the same shift that occurs as the stutter is traversed, as a result of an extensively underwound coiled coil. Residues in these trimeric coiled coils, therefore, cannot be precisely designated by heptad positions *a, b, c, d, e, f,* or *g* nor be designated as located solely in *d/a* or *a/d* (x) layers, but would appear to require a more continuous and graded designation. This continuity creates more layers with potential non-close-packed character than was previously recognized.

FUNCTIONAL ASPECTS

α-Helical coiled-coil domains display great diversity in length and play a variety of structural and dynamic roles in many proteins. In some transcription factors, for example, relatively short stretches of coiled coil (e.g., four heptads) are sufficient to effect dimerization. In these proteins, the heptad repeat is uninterrupted and only knobs-into-holes packing is generally found at the interface between the helices.[1] By contrast, in many other α-fibrous proteins, the coiled-coil domains are longer (up to ~1500 Å) and conserved heptad breaks are distributed throughout their length. The model we have advanced to account for the heptad phase discontinuities relates to two important features of such structures: destabilization of the coiled coil produced by non-close-packed cores, and global repositioning of distant residues resulting from the underwinding (or overwinding) of the supercoil.

Weak interhelical contacts, such as those in non-close-packed cores, may affect the integrity of the coiled coil in a number of different ways. In the case of short coiled coils, these regions may cause the helices to dissociate from one another unless other stabilizing domains are present. For example, the rat mannose-binding protein discussed above includes a highly nonhelical carbohydrate-binding domain attached to the $4\frac{1}{2}$-heptad long triple-stranded coiled coil. Circular dichroism studies show a disappearance of the helical signal in a proteolyzed fragment missing the carbohydrate-binding domain.[47] Since the N-terminal three heptads contain apolar residues (isoleucine, leucine, and methionine) in the core *a* and *d* positions,[47] the *d/a* layer present at the C terminus may contribute to the destabilization of the structure. This effect is analogous to the instability of extremely short coiled coils, such as that displayed by the two-heptad N-terminal fragment of GAL4, which cannot dimerize unless bound to DNA,[49] and contrasts with the stability of structures with well-packed cores, such as GCN4.[1]

Just as certain types of capping residues (such as proline, which interrupts main-chain hydrogen bonding) are found at or near the termini of α helices in globular proteins,[50] local destabilization may also play a role in the termination of a coiled coil. Inspection of the influenza hemagglutinin structure (both in the neutral[12] and low pH[45] forms) (S. Watowich and F. Hughson, personal communications), for example, shows that the last heptad of the coiled coil forms non-close-packed *a/d* and *d/a* layers, respectively, at HA_2 residues 102 (leucine) and 105/106 (glutamine/histidine), as discussed earlier. Note that the *a/d* layer may be especially destabilizing, since only one side chain from each helix contacts the others (Fig. 5C, right). After residue 106, in the

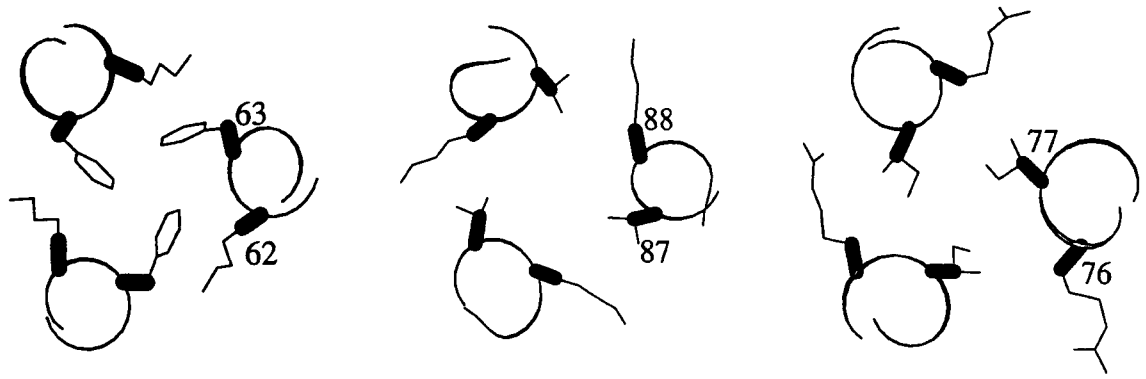

Fig. 6. Side-chain packing diagrams, similar to those in Figure 5, but highlighting the main-chain determined Cα-Cβ vectors for selected layers in the low pH form of hemagglutinin[45] (PDB code 1HTM). (Note that, structurally, the Cβ atom is part of the main chain in that its position is determined solely by the conformation of other main-chain atoms.) The Cα-Cβ vectors of residues 63 and 88 adopt similar *d/a*-type orientations relative to the facing helix (i.e., they both point more toward the outside of the coiled coil than does, for example, the Cα-Cβ vector of *a* position 77). Their side chains, however, adopt quite different conformations, resulting in an *a*-type knobs-into-holes close-packed core for phenylalanine 63.

pH neutral form of hemagglutinin, the helices splay apart and contact the fusion peptide of the molecule. In the conformation of the molecule at the low pH condition of the endosome, this region undergoes significant rearrangement, and the fusion peptide is displaced so that the virus can enter the cell.[45] Since the heptad repeat of apolar residues is observed in the sequence up to residue 125,[51,52] the non-close-packed cores at residues 102 and 105/106 may serve as coiled-coil termination signals. Similarly, side chains form a non-close-packed core at the C terminus of the mannose-binding protein coiled coil.

Although a weakened core region can affect the integrity of a relatively short coiled coil, such a defect embedded in a longer rod may be expected to cause only a local region of instability. As discussed above, with a well-packed core, about 28 residues are probably required to form a stable coiled coil,[1] but in many of the long fibrous proteins (e.g., myosin, paramyosin, and intermediate filaments) the cores are often imperfect. Here, certain "hot spots," which can be regions of small/charged residues occupying *a* and *d* positions, or the non-close-packed cores at heptad discontinuities, may serve as points of flexibility. A striking example of this effect is found in myosin, where the location of three of the four well-separated skip residues[53] (also see Table I) correlate with bends in the approximately 1,500-Å rod as seen in electron micrographs.[54] Flexibility is also observed in bacterial M protein, where a subdomain including six closely spaced discontinuities separates two long stretches of uninterrupted heptad repeats.[20]

Although breaks in the heptad substructure may coincide with regions of weakened interhelical interaction, this need not be the case. In the model presented here, heptad phase shifts are accommodated by underwinding (or overwinding) the coiled-coil main chain. Thus, although the Cα-Cβ vectors are so positioned that side chains could interact to produce non-close-packed cores, variations in the types of side chains and side-chain conformations, combined with other adjustments to the coiled-coil main chain (such as radius and local pitch[55]) could allow knobs-into-holes stabilization to be recovered. In the low pH form of hemagglutinin,[45] for example, phenylalanine 63 and lysine 88 are at the sites of stutters, and their main chains are in positions to form *d/a*-type layers (Fig. 6). Here, the lysine 88 side chain points toward the surface of the coiled coil and participates in a non-close-packed core, but phenylalanine 63 is oriented differently so that its apolar side chain points back into the interior of the coiled coil, thus participating in a knobs-into-holes-type core.

The use of apolar side chains at the sites of heptad phase shifts may indeed be a way in which some proteins retain significant stability. Omp α from the thermophilic *Thermotoga maritima* is an unusually stable coiled coil, although it is predicted to contain about 8 *d/a* layers (Fig. 1a in ref. 8; also see Table I), which accommodate the drift in the heptad phase. Although some of the stability of this long protein may arise from the large interhelical contact area of its predicted four-stranded coiled coil, another source may be the high occurrence of apolar residues at the *d/a* layers. In all eight predicted *d/a* layers, hydrophobic residues are found in at least one of the core positions, and in three of the layers, they are found in both positions. One might expect that many of these side chains—as shown for phenylalanine 63 of hemagglutinin—would be sequestered in the core and consequently form knobs-into-holes-type structures.

Regardless of whether destabilizing non-close-packed cores are formed, the under- or overwinding

of the supercoil required in our model for accommodating stutters and stammers respectively, has implications for a wide variety of α-fibrous proteins. α-Helical coiled coils generally terminate in nonhelical domains.[6] As described earlier, the effect of the local pitch changes will propagate along the coiled coil to alter the relative disposition of residues at the beginning and end of the protein. This global effect is analogous to the insertion of a one-residue β bulge into a β strand[56] which, by altering the twist between neighboring strands, changes the relative disposition of opposite sides of the β sheet. (In contrast, such an insertion into a loop region between secondary structural elements generally has only local effects on the protein structure.) We should note, however, that modulations in the pitch of the coiled coil are also observed in tropomyosin,[57] although its heptad repeat is uninterrupted. In addition to heptad phase shifts, specific residues may produce such changes. Heptad phase shifts may, however, provide a systematic method of effecting them.

An additional important consequence of this global effect would be the alteration of the azimuthal position of the periodic patches of charged and/or apolar residues along the coiled coil that are known to play a primary role in the aggregation of some α-fibrous proteins into filamentous assemblies.[6] Thus the formation of specific aggregates in proteins such as myosin, paramyosin, and intermediate filaments, are undoubtedly modulated by the conserved stutters that characterize these heptad repeats. These considerations also suggest it may be possible to engineer appropriate frame shift mutations into α-fibrous proteins that will modify the positions of key residues in a predictable manner, so that different sets of interactions important either for aggregation or function can be brought into play. We anticipate that the discovery of additional fundamental roles carried out by discontinuities in the heptad phasing in α-fibrous proteins will stimulate the creativity of protein engineers and provide new insights into the complex relationship between amino acid sequence and the higher levels of structure adopted by this diverse class of proteins.

ACKNOWLEDGMENTS

This work was supported by grants to C.C. from the National Institutes of Health (AR17346) and the Muscular Dystrophy Association. J.H.B. is a Postdoctoral Fellow of the Medical Foundation and is supported by Fleet Bank of Massachusetts, N.A., Trustee of the Charles A. King Trust.

REFERENCES

1. O'Shea, E.K., Klemm, J.D., Kim, P.S., Alber, T. X-ray structure of the GCN4 leucine zipper, a two-stranded, parallel coiled coil. Science 254:539–544, 1991.
2. Harbury, P.B., Zhang, T., Kim, P.S., Alber, T. A switch between two-, three- and four-stranded coiled coils in GCN4 leucine zipper mutants. Science 262:1401–1407, 1993.
3. Harbury, P.B., Kim, P.S., Alber, T. Crystal structure of an isoleucine-zipper trimer. Nature 371:80–83, 1994.
4. Conway, J.F., Parry, D.A.D. Three-stranded α-fibrous proteins: The heptad repeat and its implications for structure. Int. J. Biol. Macromol. 13:14–16, 1991.
5. Pauling, L., Corey, R.B. Compound helical configurations of polypeptide chains: Structure of proteins of the α-keratin type. Nature 171:59–61, 1953.
6. Cohen, C., Parry, D.A.D. α-helical coiled coils and bundles: How to design an α-helical protein. Proteins 7:1–15, 1990.
7. Crick, F.H.C. The packing of α-helices: Simple coiled coils. Acta Crystallogr. 6:689–697, 1953.
8. Lupas, A. Müller, S., Goldie, K., Engel, A.M., Engel, A., Baumeister, W. Model structure of the Ompα rod, a parallel four-stranded coiled coil from the hyperthermophilic eubacterium *Thermotoga maritima*. J. Mol. Biol. 248:180–189, 1995.
9. Parry, D.A.D. Fibrinogen: A preliminary analysis of the amino acid sequences of the portions of the α,β, and γ-chains postulated to form the interdomainal link between globular regions of the molecule. J. Mol. Biol. 120: 545–551, 1978.
10. Berger, B., Wilson, D.B., Wolf, E., Tonchev, T., Milla, M., Kim, P.S. Predicting coiled coils by use of pairwise residue correlations. Proc. Natl. Acad. Sci. U.S.A. 92:8259–8263, 1995.
11. Weis, W., Brown, J.H., Cusack, S., Paulson, J.C., Skehel, J.J., Wiley, D.C. Structure of the influenza virus haemagglutinin complexed with its receptor, sialic acid. Nature 333:426–431, 1988.
12. Wilson, I.A., Skehel, J.J., Wiley, D.C. Structure of the haemagglutinin membrane glycoprotein of influenza virus at 3 Å resolution. Nature 289:366–373, 1981.
13. North, A.C.T., Steinert, P.M., Parry, D.A.D. Coiled-coil stutter and link segments in keratin and other intermediate filament molecules: A computer modeling study. Proteins 20:174–184, 1994.
14. Karn, J., Brenner, S., Barnett, L. Protein structural domains in the *Caenorhabditis elegans* unc- 54 myosin heavy chain gene are not separated by introns. Proc. Natl. Acad. Sci. U.S.A. 80:4253–4257, 1983.
15. Kagawa, H., Gengyo, K., McLachlan, A.D., Brenner, S., Karn, J. The paramyosin gene (unc-15) of *Caenorhabditis elegans:* Molecular cloning nucleotide sequence and models for thick filament assembly. J. Mol. Biol. 207:311–333, 1989.
16. Geisler, N., Kaufman, E., Weber, K. Protein chemical characterization of three structurally distinct domains along the protofilament unit of desmin 10 nm filaments. Cell 30:277–286, 1982.
17. Peter, M., Kitten, G.T., Lehner, C.F., Vorburger, K., Bailer, S.M., Maridor, G., Nigg, E.A. Cloning and sequencing of cDNA clones encoding chicken lamins A and B_1 and comparison of the primary structures of vertebrate A- and B-type lamins. J. Mol. Biol. 208:393–404, 1989.
18. Tanaka, T., Parry, D.A.D., Klaus-Kovtun, V., Steinert, P.M., Stanley, J.R. Comparison of molecularly cloned bullous pemphigoid antigen to desmoplakin I confirms that they define a new family of cell adhesion junction plaque proteins. J. Biol. Chem. 266:12555–12559, 1991.
19. Wiche, G., Becker, B., Luber, K., Weitzer, G., Castanon, M.J., Hauptaman, R., Stratowa, C., Stewart, M. Cloning and sequencing of rat plectin indicates a 466 kD polypeptide chain with a three-domain structure based on a central alpha-helical coiled coil. J. Cell Biol. 114:83–99, 1991.
20. Fischetti, V.A., Parry, D.A.D., Trus, B.L., Hollingshead, S.K., Scott, J.R., Manjula, B.N. Conformational characteristics of the complete sequence of group A streptococcal M6 protein. Proteins 3:60–69, 1988.
21. Leung, E., Print, C.G., Parry, D.A.D., Closey, D.N., Skinner, S.J.M., Batchelor, D.C., Krissansen, G.W. A new gene family of coiled-coil proteins: Cloning of mouse CG-1 and its relatedness to ES/130 and kinectin. J. Immun. and Cell Biol. (in press).
22. Parry, D.A.D. NuMa/centrophilin: Sequence analysis of the coiled-coil rod domain. Biophys. J. 67:1203–1206, 1994.
23. Mirzayan, C., Copeland, C.S., Snyder, M. The NUF1 gene

encodes an essential coiled-coil related protein that is a potential component of the yeast nucleoskeleton. J. Cell Biol. 116:1319–1332, 1992.
24. Osborne, M.A., Schlenstedt, G., Jinks, T., Silver, P.A. Nuf2, a spindle pole body-associated protein required for nuclear division in yeast. J. Cell Biol. 125:853–866, 1994.
25. Page, B.D., Snyder, M. CIK1: A developmentally regulated spindle pole body-associated protein important for microtubule function in *Saccharomyces cerevisiae*. Gene Dev. 6:1414–1429, 1992.
26. Kosik, K.S., Orecchio, L.D., Schnapp, B., Inouye, H., Neve, R.L. The primary structure and analysis of the squid kinesin heavy chain. J. Biol. Chem. 265:3278–3283, 1990.
27. Garber, A.T., Retief, J.D., Dixon, G.H. Isolation of dynein heavy chain cDNAs from trout testis which predict an extensive carboxyl-terminal alpha-helical coiled-coil domain. EMBO J. 8:1727–1734, 1989.
28. Doxsey, S.J., Stein, P., Evans, L., Calarco P.D., Kirschner, M. Pericentrin, a highly conserved centrosome protein involved in microtubule organization. Cell 76:639–650, 1994.
29. Weber, K., Geisler, N., Plessmann, U., Bremerich, A., Lechtreck, K-F., Melkonian, M. SF-assemblin, the structural protein of the 2-nm filaments from striated microtubule associated fibers of algal flagellar roots, forms a segmented coiled coil. J. Cell Biol. 121:837–845, 1993.
30. Cole, D.G., Chinn, S.W., Wedaman, K.P., Hall, K., Vuong, T., Scholey, J.M. Novel heterotrimeric kinesin-related protein purified from sea urchin eggs. Nature 366:268–270, 1993.
31. Holberton, D., Baker, D.A., Marshall, J. Segmented α-helical coiled-coil structure of the protein giardin from the giardia cytoskeleton. J. Mol. Biol. 204:789–795, 1988.
32. Marshall, J., Holberton, D.V. Sequence and structure of a new coiled-coil protein from a microtubule bundle in giardia. J. Mol. Biol. 231:521–530, 1993.
33. Marshall, J., Holberton, D.V. Giardia gene predicts a 183 kDa nucleotide-binding head-stalk protein. J. Cell Sci. 108:2683–2692, 1995.
34. Nair, J., Müller, H. Peterson, M. and Novick, P. Sec2 protein contains a coiled-coil domain essential for vesicular transport and a dispensable carboxy terminal domain. J. Cell Biol. 110:1897–1909, 1990.
35. Strunnikov, A.V., Larionov, V.L., Koshland, D. SMCI: An essential yeast gene encoding a putative head-rod-tail protein is required for nuclear division and defines a new ubiquitous protein family. J. Cell Biol. 123:1635–1648, 1993.
36. Sobolev, B.N., Mesyanzhinov, V.V. The Wac gene product of bacteriophage T4 contains coiled-coil structural patterns. J. Biomol. Struct. Dynamics 8:953–965, 1991.
37. Fraser, R.D.B., Furlong, D.B., Trus, B.L., Nibert, M.L., Fields, B.N., Steven, A.C. Molecular structure of the cell-attachment protein of reovirus: Correlation of computer-processed electron micrographs with sequence-based predictions. J. Virol. 64:2990–3000, 1990.
38. Koski, P., Saarilahti, H., Sukupolvi, S., Taira, S., Riikonen, P., Österlund, K., Hurme, R., Rhen, M. A new α-helical coiled-coil protein encoded by the *Salmonella typhimurium* virulence plasmid. J. Biol. Chem. 267: 12258–12265, 1992.
39. Nakajima, H., Hirata, A., Ogawa, Y., Yonehara, T., Yoda, K., Yamasaki, M. A cytoskeleton-related gene, USO1, is required for intracellular protein transport in *Saccharomyces cerevisiae*. J. Cell Biol. 113:245–260, 1991.
40. Ainscough, R. (submitted to EMBL Data Library, April 1994, Accession S43597).
41. Wharton, R.P., Struhl, G. Structure of the *Drosophila bicaudalD* protein and its role in localizing the posterior determinant *nanos*. Cell 59:881–892, 1989.
42. Mitchell, P.J., Cooper, C.S. The human tpr gene encodes a protein of 2094 amino acids that has extensive coiled-coil regions and an acidic C-terminal domain. Oncogene 7:2329–2333, 1992.
43. Seo, J., Cohen, C. Pitch diversity in α-helical coiled coils. Proteins 15:223–234, 1993.
44. Stebbins, C.E., Borukhov, S., Orlova, M., Polyakov, A., Goldfarb, A., Darst, S.A. Crystal structure of the GreA transcript cleavage factor from *Escherichia coli*. Nature 373:636–640, 1995.
45. Bullough, P.A., Hughson, F.M. Skehel, J.J., Wiley, D.C. Structure of influenza haemagglutinin at the pH of membrane fusion. Nature 371:37–43, 1994.
46. Phillips, G.N., Jr. What is the pitch of the α-helical coiled coil? Proteins 14:425–429, 1992.
47. Weis, W.I., Drickamer, K. Trimeric structure of a C-type mannose-binding protein. Structure 2:1227–1240, 1994.
48. Sheriff, S., Chang, C.Y., Ezekowitz, A.B. Human mannose-binding protein carbohydrate recognition domain trimerizes through a triple α-helical coiled coil. Struct. Biol. 1:789–793, 1994.
49. Marmorstein, R., Carey, M., Ptashne, M., Harrison, S.C. DNA recognition by GAL4: Structure of a protein-DNA complex. Nature 356:408–414, 1992.
50. Richardson, J.S., Richardson, D.C. Amino acid preferences for specific locations at the ends of α helices. Science 240: 1648–1652, 1988.
51. Carr, C.M., Kim, P.S. A spring-loaded mechanism for the conformational change of influenza hemagglutinin. Cell 73:823–832, 1993.
52. Ward, C.W., Dopheide, T.A. Influenza virus haemagglutinin: Structural predictions suggest that the fibrillar appearance is due to the presence of a coiled coil. Aust. J. Biol. Sci. 33:441–447, 1980.
53. McLachlan, A.D., Karn, J. Periodic features in the amino acid sequence of nematode myosin rod. J. Mol. Biol. 164: 605–626, 1983.
54. Offer, G. Skip residues correlate with bends in the myosin tail. J. Mol. Biol. 216:213–218, 1990.
55. Offer, G., Sessions, R. Computer Modelling of the α-helical coiled coil: Packing of side-chains in the inner core. J. Mol. Biol. 249:967–987, 1995.
56. Richardson, J.S., Getzoff, E.D., Richardson, D.C. The β-bulge: A common small unit of nonrepetitive protein structure. Proc. Natl. Acad. Sci. U.S.A. 75:2574–2578, 1978.
57. Phillips, G.N., Jr., Fillers, J.P., Cohen, C. Tropomyosin crystal structure and muscle regulation. J. Mol. Biol. 192: 111–131, 1986.